

DRY-STACKED MASONRY SUBJECTED TO ULTIMATE LOADS

Gero A. Marzahn¹

Abstract

Dry-stacked masonry without any mortar between the blocks is accomplished by laying blocks dry upon each other. This kind of brickwork does not only save costs, and therefore, may be an interesting topic for low cost housing, but it also offers a load-carrying capacity nearly to the same extent as traditional masonry with mortar joints. Because of the limited knowledge on the structural behavior and prejudice as well, dry-stacked masonry has not found a wide application yet. In order to systematically enhance the knowledge about mortarless masonry, several structural tests were conducted. This paper reports on those tests of dry-stacked masonry subjected to an entire spectrum of loads: compression, shear, and bending parallel and perpendicular to bed joints.

1 Introduction

Dry-stacked masonry differs from traditional masonry in that no mortar is used to build up brickwork. The units, usually the same as those used for masonry with a thin mortar layer, are laid dry upon each other. Despite the fact that failure mechanisms are altered by the lack of mortar, dry-stacked masonry has nearly the same load-bearing capacity as mortared masonry.

2 Constituent Masonry Blocks

Two different types of masonry blocks each represented by two blocks of different strength were used: calcium silicates (CS1, CS2) and autoclaved aerated concrete blocks (AAC1, AAC2). The main properties of these blocks are summarized in table 1 and were gathered by standardized test procedures except for the uniaxial compressive strength. Different from the unit compressive strength, where entire units were tested, the uniaxial compressive strength was obtained from small cylinders drilled out from blocks and subjected to a displacement-controlled compression load. By means of this test procedure not only the entire load-displacement behavior could be monitored, but also the compressive strength could be determined independent of slenderness influences. Vice versa, the axial tensile strength was obtained on similar cylinders subjected to direct tension, and also marks a uniaxial strength value.

¹ Dr.-Ing., University of Leipzig, Institute for Structural Materials, 04109 Leipzig, Germany and KHP Consulting Engineers, Leipzig, Germany

Table 1 Unit Properties, mean values
(1 inch = 25.4 mm, 1 psi = 0.0069 N/mm², 1 lb/ft³ = 0.016 kg/dm³)

Quantity		Calcium silicates		Autoclaved aerated concrete	
		CS1	CS2	AAC1	AAC2
Depths L/W/H	mm	500 / 240 / 238		500 / 240 / 200	
Density	kg/dm ³	1.857	1.864	0.544	0.450
Unit compressive strength	N/mm ²	25.90	20.91	4.11	3.21
Uniaxial compressive strength	N/mm ²	17.10	12.78	3.85	2.79
Axial tensile strength	N/mm ²	1.42	1.56	0.95	0.46

3 Compression Tests

The compression behavior of dry-stacked masonry was observed during three test series.

3.1 First Test Series

The first series compared the load carrying behavior of dry-stacked and thin mortar layer masonry. Unlike thin mortar layer masonry (appr. 1 mm thick mortar joints), dry-stacked masonry is currently not standardized neither in Germany nor in Europe. Hence, mortared masonry specimens were needed to have anchor values to which comparisons could be made. Small wall specimens (Figure 1) of either dry-stacked or thin mortar layer masonry of all four kinds of blocks (in all more than 24 tests) were gradually subjected to compression (load-controlled test scheme). Unlike that of the mortared masonry, the failure of dry-stacked masonry did not manifest as a splitting in its plane but rather as cracks starting at the edges and running diagonally across the specimen from corner to corner, initiating a shear failure along these cracks. Unexpectedly, the crack direction was not influenced by the masonry's joints; rather, the dry-stacked masonry behaved and finally failed as would a homogeneous material such as concrete (Figure 2).

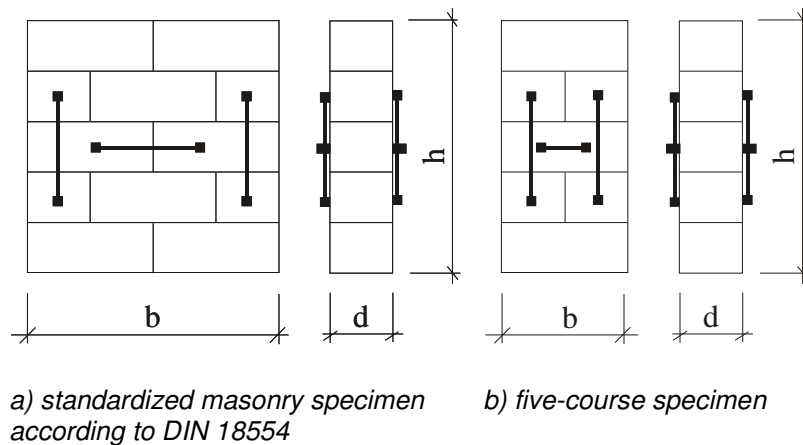


Figure 1 Specimen for compression tests

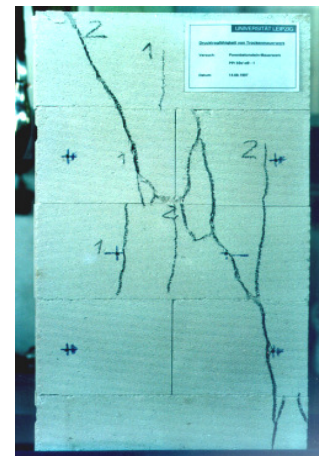


Figure 2 Crack pattern

Stresses and strains were continuously monitored. Whereas the stress-strain relationship of the mortared masonry had a common convex shape, that of the dry-stacked masonry showed two characteristic parts: the first, lower concave part was mainly influenced by the joint settlement, and the second, upper convex part was predominantly determined by the material itself (Figure 3). A settlement of the experimental setup can be excluded because it was trained at very low load levels.

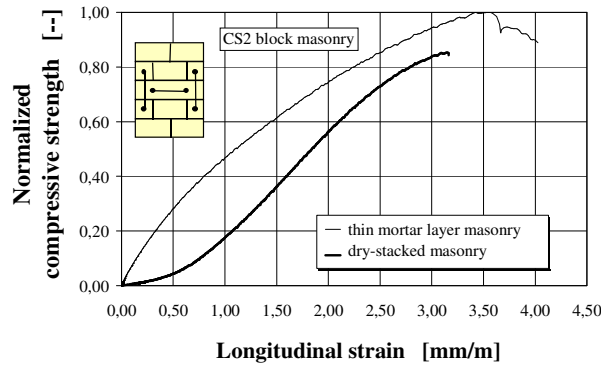


Figure 3 Comparison of stress-strain relationships

The turning point between the two curves can be fixed at approximately one-third of the ultimate strength (Figure 4). The elastic modulus must, therefore, have to be defined for each part of the curve separately. In the second, or upper, part where the material is principally stressed, the elastic modulus can be determined by a secant through the points that equal one-third and two-thirds of the ultimate strength f and their corresponding strains ϵ_{33} and ϵ_{66} . It is called $E_{33/66}$. $E_{33/66}$ gained magnitudes of 5,000 to 7,000 MPa for CS specimens and 1,100 to 1,700 MPa for AAC specimens. By means of a linear relationship, the elastic modulus $E_{33/66}$ can be predicted using the masonry compressive strength (Marzahn 2000):

$$E_{33/66} = 450 \cdot f \quad \text{for CS masonry} \quad (1)$$

$$E_{33/66} = 471 \cdot f \quad \text{for AAC masonry} \quad (2)$$

with: $E_{33/66}$ secant modulus, f compressive masonry strength.

In the first or lower part, where the joint settlement dominates, the elastic modulus is only a fraction of $E_{33/66}$, varying between one-tenth and one-fifth of $E_{33/66}$.

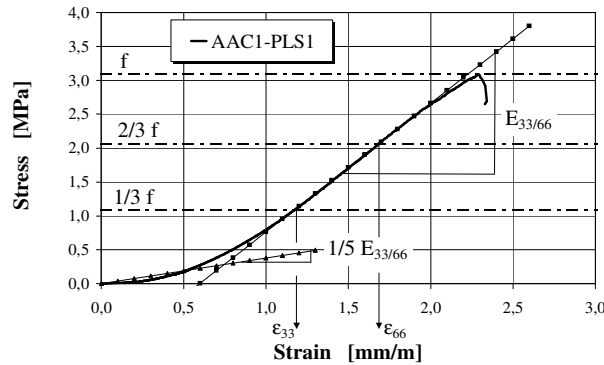


Figure 4 Determination of the elastic modulus of dry-stacked masonry

It was observed that the overall compressive strength of mortarless masonry was slightly lower (at most 15 percent lower) than that of thin mortar layer masonry (Table 2). The elastic modulus followed in the same way. The compressive strength was proved to be almost independent of the accuracy of the bedding faces of the blocks, but the question of how well the blocks fit together had a great impact on deformation. The greater the surface roughness, the greater the settlement of joints. The lower compressive strength of dry-stacked masonry was seen primarily in the early cracks of the mortarless structures, which may occur soon after loading and are caused by inaccurate fitting in the bed joints. Spalling was not observed. Consequently, it can be understood that the failure mechanism was changed by the lack of mortar.

Upon closer examination, one can see that the settlement phenomenon is due to the settlement of the contact surfaces between the blocks. In Figure 5, a bed joint detail

before and after loading is depicted. Due to the roughness and the asperities of the surfaces, the small contact areas first lead to stress localization, which is much higher than the applied stress. If the concentrated stress exceeds the strength of the material, a partial crushing may occur. The rough surfaces thus become more even, the contact areas grow, and the height of the specimens shrinks. This continues until the total contact area is large enough to safely transfer the stresses across the joint. The compaction of joints is generally referred to as joint settlement.

*Table 2 Compression properties of dry-stacked masonry, mean values
(1 psi = 0.0069 N/mm²)*

Block	Compressive strength f N/mm ²	Longitudinal strain under maximum stress ϵ_{m1} mm/m	Elastic modulus $E_{33/66}$ N/mm ²	Poisson's ratio ν_{33} —
CS1	12.12	3.02	5,627	0.31
CS2	12.44	3.75	5,276	0.34
AAC1	2.34	3.14	1,455	0.22
AAC2	1.96	3.14	881	0.10

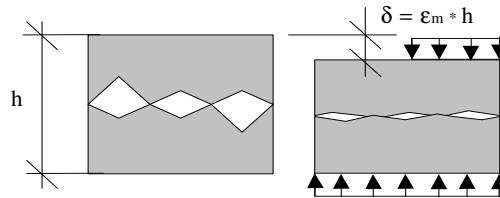


Figure 5 Joint settlement

In order to observe this flattening of the joint, a thin paper sheet was placed between two separate blocks, and the two-course specimen was subjected to a small load. The paper was removed and visually evaluated, then again placed between the blocks, and a higher load was applied. Under the small load, only 60 to 80 percent of the nominal joint area was actually in contact, but when subjected to a higher load, the contact area grew to greater than 90 percent. Thus, it is clear that most of the deformations obtained were joint related and obviously occurred inelastically.

3.2 Second Test Series

To study the influence of bedding quality, a second test series was conducted. Blocks (CS1, CS2, AAC1, AAC2) with specifically worked bedding faces were arranged as five-course specimens (Figure 1b) and subjected to a compression load.

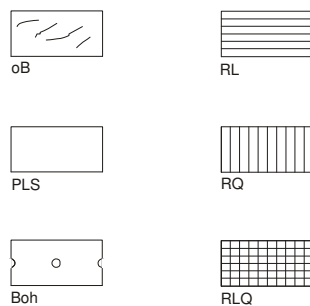


Figure 6 Specifically worked bedding faces of test blocks

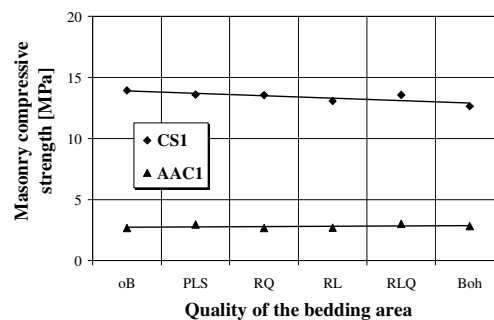


Figure 7 Masonry compressive strength

The bedding areas of the blocks were left unworked (oB), polished (PLS), or were specifically damaged with small notches cut parallel (RL) and/or perpendicular to the block length (RLQ/RQ) (Figure 6). It was found that the quality of the bedding face affected the deformation rather than the compressive strength. The lowest strength values were some 7 percent below those of unworked or even polished blocks and did not necessarily refer to the blocks with the most damaged bedding areas (Figure 7).

3.3 Third Test Series

A third test series sought to investigate the influence of a growing number of dry bed joints on the bearing and deformation capacity of dry-stacked masonry. For this reason, specimens varying in height from one to five courses were subjected to a compression load. The vertical compaction was measured by means of strain gauges over one block and also with linear variable differential transformers (LVDTs) over the total height.

The bedding areas of the blocks were not specifically worked. The loading impact was designed to load and unload the specimens three times before the ultimate load magnitude was reached. The upper cyclic stress varied between 1.0 MPa for AAC units and 3.0 MPa for CS units and was expected to be about one-third of the ultimate load level. The low load level was chosen to avoid nonproportional deformation within the block material and, therefore, to assign all occurring plastic strains to the bed joints. Figure 8 illustrates, for example, the stress-strain relationship of the CS2 specimens.

The strength results showed that the strength dropped as the specimen height grew. This is primarily caused by a growing slenderness ratio, reaching from about $\lambda = 1.0$ to about $\lambda = 5.0$. The effect of second order deformation may be eliminated, so that at a slenderness of $\lambda = 3.0$ did not drop further (arrival at uniaxial masonry compressive strength). A significant influence of a higher portion of bed joints in mortarless masonry on the compressive strength was not observed (Marzahn 2000). Due to the low load impact, all blocks behaved similarly and entirely elastically.

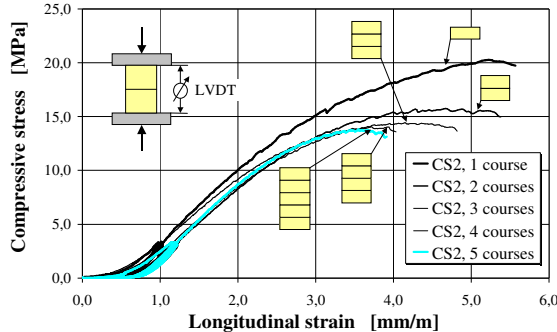


Figure 8 Stress-strain diagram of dry masonry depending on specimen height

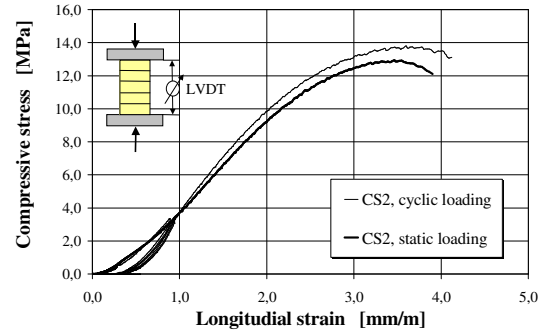


Figure 9 Comparison of stress-strain relationship at static and cyclic loading

The five-course specimen experienced the most strain gain under the same load. Consequently, it can be assumed that if more bed joints experience a settlement, it will add up to a greater deformation for the whole specimen. Most of the accrued deformation is plastic and permanent, remaining even after the load is removed. The cycled loading also provided the opportunity to see that the joint settlement primarily occurred at first loading because the unloading path intersected the strain-axis beyond the origin. A second cycle contributed much less, and a third cycle was actually insignificant as long as the previous load level was not exceeded. The loading and unloading paths began to overlay each other in the end, but they were steeper than the first loading path (Figure 8). This is a sign that the joints gained stiffness due to compaction. But once the former load level was surpassed, the masonry behaved as if it were in the first loading cycle for the new load level. Then there are not any differences between cyclic and static loading (Figure 9).

4 Shear Tests

For testing shear strength, four full-scale tests were performed using CS2 and AAC1 blocks for two tests each. The advantages of full-scale testing are that all influences that might occur in a real shear wall are covered by this test setup. Very important for this test was to impact the load in such a manner that the generated shear stresses were evenly distributed across the wall. Therefore, the test focused on a quadratic wall with an edge length measuring 2.50 m, which can be thought of as an enlarged finite element being uniformly subjected to constant shear stresses on its edges (Figure 10).

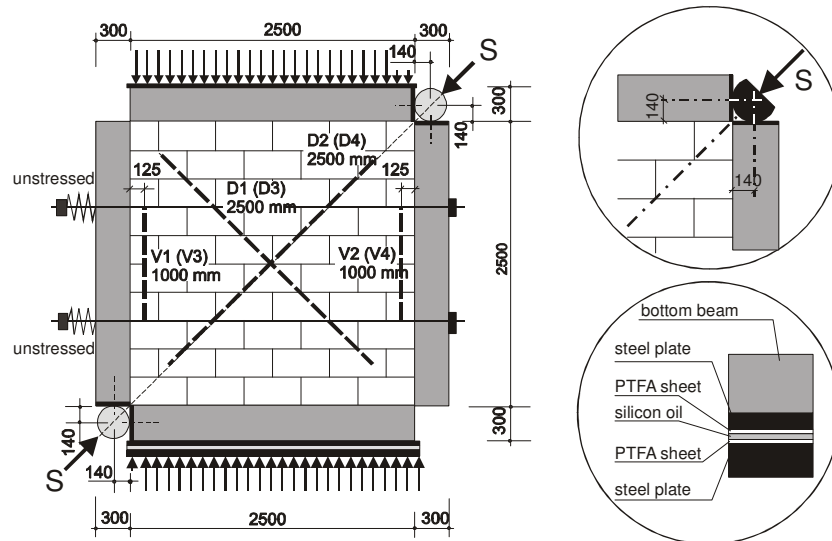


Figure 10 Shear wall test setup

Besides the vertical precompression, a diagonal compression force was displacement-control applied to the tops of the concrete beams that were glued on each edge of the wall. The stressed concrete beams ensured a uniform shear stress distribution over the panel (Figure 11). The vertical precompression was applied externally using a fixed jack on the top of the wall. The magnitude of the precompression force was chosen to equal stresses of 0.50 and 0.80 MPa for CS2 blocks and 0.33 and 0.50 MPa for AAC1 blocks. To avoid the edge beams on the sides being prestressed, they were glued into place after the precompression was applied. For safety reasons, the side beams were additionally attached by barely stressed horizontal steel rods. The entire test setup was isolated from the ground by a frictionless PTFA sheet to ensure that the shear forces were confined to the system and did not move into the ground. The deformations in diagonal and vertical directions on each side of the wall were measured by means of LVDTs.

The first cracks appeared at the loaded corners at an angle of about 45 degrees, but developed more vertically as they ran more deeply into the wall. The cracks at the corners were initiated by shear stresses but drifted vertically through the overlay due to vertical precompression. The higher the precompression, the sooner the vertical crack orientation occurred. Despite these first cracks, the shear capacity of the mortarless masonry was not exhausted at this point, although the stiffness was lowered, leading to a growing degradation. Finally, the cracks appeared concentrated along the stressed diagonal of the wall but were principally vertically oriented (Figure 11). This means that the orientation of the principal stresses, if the wall is seen as a homogeneous model, was predominantly influenced by the vertical precompression rather than the shear stresses leading to vertically adjusted principal compression and horizontally adjusted principal tension, which was also proved by a finite element analysis.

As can be seen in Figure 12 for the CS2 walls, the shear stresses versus diagonal strains developed symmetrically for tension and compression. With augmented

distortion, the tensile strains grew somewhat faster than the compressive ones, which might be caused by cracks and initial sliding in the bed joints. A higher precompression enhanced the ultimate shear load, due to higher friction in the joints (table 3), but not the stiffness of the wall. Whereas the strength increase numbered 65 to 70 percent depending on the blocks and prestressing, the related distortion grew by almost 100 percent.



Figure 11 Crack pattern after conducting the test

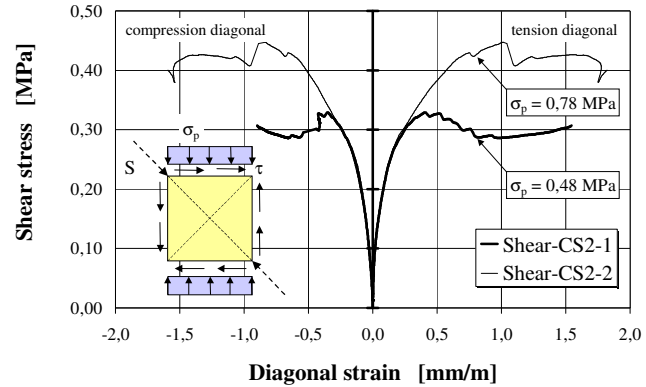


Figure 12 Shear stress-distortion relationship of CS2 shear walls under varying precompression

Depending on the precompression, two failure mechanisms were observed: first, a sliding along the bed joints leading also to a flattening of the dry joints at lower precompression, and second, cracks running through joints and blocks at higher precompression. Neither of these failures occurred abruptly, but instead gradually stabilized the shear load at a residual and nearly constant friction level.

Table 3 Shear test results (1 psi = 0.0069 N/mm²)

		Shear wall CS1-1	Shear wall CS1-2	Shear wall AAC1-1	Shear wall ACC1-2
Initial precompression	N/mm ²	0.480	0.776	0.326	0.473
Shear strength	N/mm ²	0.329	0.447	0.203	0.274
Diagonal lengthening ¹⁾	mm/m	0.413	1.016	1.148	3.307
Diagonal shortening ¹⁾	mm/m	0.355	0.837	0.554	2.068

1) at maximum stresses

It should also be noted that sliding leads to a vertical dilatation because the asperities slide upon each other, which vertically expands the wall. If the dilatation is restrained by precompression, it will enhance the prestressing action and the friction resistance of the joints. For high precompression, the material strength rather than the friction may become decisive when the asperities are leveled and eliminated by a sliding movement, but both must be taken into account for design purposes

5 Bending Tests

5.1 Bending Parallel to Bed Joints

The bending strength of masonry depends on the direction of the load impact, which can be parallel or perpendicular to the bed joints. For bending stresses parallel to bed joints, the resistance of the joints is primarily decisive, and a prestressing perpendicular to the joints improves the bearing capacity by enhancing the friction in the joints. Depending on the prestressing force, either a sliding out of the panel or a cracking through the blocks may occur. For the test, two walls made of CS2 blocks and two of

AAC1 blocks, respectively, were supported and horizontally loaded to conduct a four-point bending test (Figure 13).

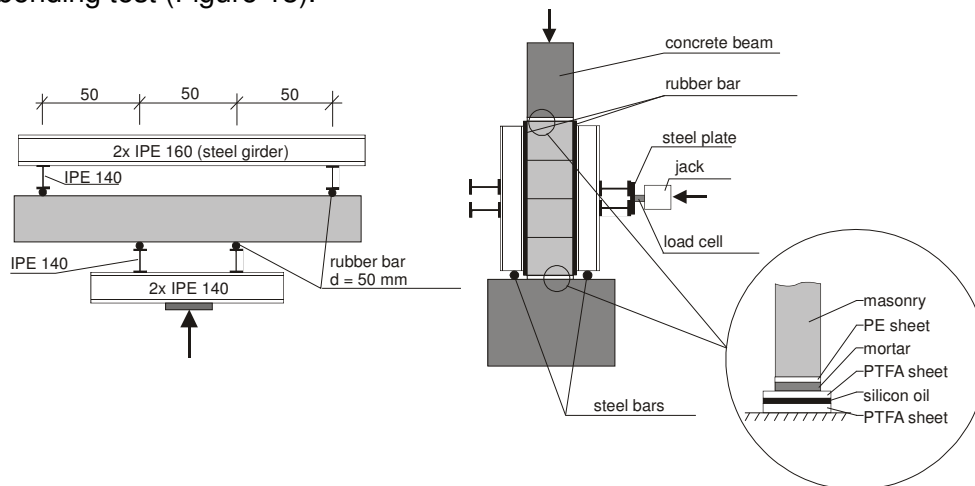


Figure 13 Test setup for bending parallel to bed joints

The vertical prestressing was applied externally using a loading frame and was kept constant during the test at a level of 0.30 and 1.85 MPa (CS2) and 0.20 and 0.90 MPa (AAC1), respectively. The horizontal bending force was increased steadily until the failure occurred. In order to avoid any restraining action between the load plates and the bottom and the top of the walls, two PTFA sheets were used to allow the wall to bend freely. All loads were monitored by load cells, and the deflection was measured by LVDTs twice along the wall length.

Table 4 Test results of bending parallel to bed joint
(1 inch = 25.4 mm, 1 psi = 0.0069 N/mm²)

		Wall CS2-1	Wall CS2-2	Wall AAC1-1	Wall AAC1-2
Initial precompression	N/mm ²	0.312	1.858	0.196	0.881
Flexural strength	N/mm ²	0.95	1.89	1.17	1.74
Midspan deflection	mm	1.36	0.76	1.63	0.83
Failure	—	joint	block	joint	block

Test results (table 4) show that at lower precompression the friction resistance in the joints was exceeded, causing the uncracked blocks in the middle of the wall to turn out. The wall with higher precompression did fail abruptly after the middle blocks cracked, though no sliding failure was visible. Due to high precompression, the initiated bending deflection of horizontal loads was much lower even though the bending stresses were higher. The increase in flexural strength between the two tests of each material equaled approximately 100 percent (CS2) and 50 percent (AAC1) based on prestressing ratios of 6.00 (CS2) and 4.50 (AAC1). The results demonstrate that the flexural strength parallel to bed joints is primarily governed by two failure conditions: either friction in the joints or the flexural tensile strength of the blocks. The internal friction action can be enhanced by prestressing perpendicular to the joints, but is limited by the bending capacity of the blocks. Whereas failure initiated by sliding is more ductile, cracking of the blocks is attributed to a brittle failure.

5.2 Bending Perpendicular to Bed Joints

If the wall is supported at the bottom and the top, bending stresses perpendicular to the bed joints may open the joints and cause a failure. Therefore, a vertical precompression is necessary to counteract tensile stresses. Additional compressive stresses may

be applied using post-tensioning. Several methods of post-tensioning are known (Falkner 1994), but for this test series the focus was on internal, centrally positioned monostrands fixed on the top and bottom of the wall. This arrangement of tendons had the advantage of the prestressing force not contributing to a buckling of the wall. Employing these guidelines and referring to the European standard DIN EN 1052, four specimens were built, two of CS2 blocks and two of AAC1 blocks. Each wall had a height of 10 courses leading to a slenderness ratio of 8.5 (CS2) and 10.5 (AAC1). Each second course was arranged from two half-blocks to consider the possible influence of head joints. For more convenient handling, the specimens were tipped downward by 90 degrees and laid on two PTFA sheets before they were prestressed and subjected to two horizontal loads as a four-point bending test (Figure 14).

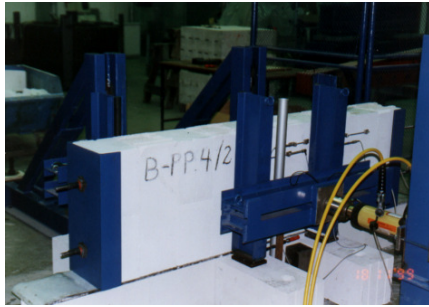
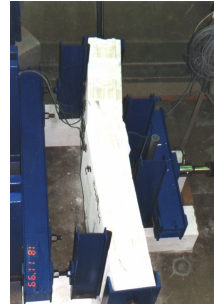
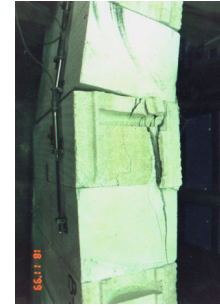


Figure 14 Test setup for bending perpendicular to bed joints



a) deflected wall



b) crushing in midspan

Figure 15 Crushing failure of a wall due to interaction of bending moments and normal forces

For the tests, prestressing levels of 0.50 and 1.00 MPa (CS2) and 0.28 MPa and 0.56 MPa (AAC1) were applied beforehand. LVDTs measured the deflection in midspan and the openings over four joints on both sides of the wall. Using these data, the curvature of the wall was computed.

Table 5 Test results of bending perpendicular to bed joints
(1 inch = 25.4 mm, 1 psi = 0.0069 N/mm²)

		Wall CS2-1	Wall CS2-2	Wall AAC1-1	Wall AAC1-2
Initial precompression	N/mm ²	0.503	1.051	0.283	0.562
Flexural strength	N/mm ²	1.742	4.237	1.536	1.715
Eccentricity ¹⁾	mm	105.22	95.15	81.91	90.05
Curvature ¹⁾	rad	0.0168	0.0570	0.0274	0.0718

¹⁾ at maximum stresses

With increasing bending loads, the deflection grew proportionally until the first joint opened. Usually, the joint in midspan opened first. With the opening of the first joint, the wall lost stiffness so that the deflection grew rapidly, leading to large joint openings of more than 20 mm. Because the neighboring joints did not follow proportionally, the deflection curve showed a sharp bend in its shape (Figure 15a). The failure was, consequently, initiated by splitting the compression zone off the cross section (Figure 15b) due to an overstressing in the axial direction. This kind of failure was observed for all walls, independent of the prestressing level. The principle difference between walls of higher and lower precompression was that the joints at higher prestressing opened later so that the bending stiffness of the wall persisted much longer, resulting in a higher failure load. Hence, prestressing greatly influenced the bending capacity, and the interaction of normal forces and bending moments

determined the failure. In table 5, the ultimate bending moments, axial forces, and flexural tensile strengths of the tested walls are outlined.

Because of the interaction of normal force N and bending moment M , several dependencies may be inferred. Based on the eccentricity and the curvature of the wall, an eccentricity-curvature relationship (e - κ -curve) can be plotted (Figure 16). Both the eccentricity and the curvature develop linearly as long as the joints are closed. With the opening of joints, the curves increasingly flatten, and the eccentricities e asymptotically approach the theoretically possible eccentricity of half of the wall thickness. Thus, it becomes clear that a higher precompression reduces the eccentricity and strengthens the compression zone to better withstand bending stresses. Plotting the curvature versus the bending moment for the AAC1 wall with a prestressing of 0.56 MPa (Figure 17) shows that moment and curvature advanced at the same rate in the beginning. The maximally stressed joints in midspan (joints 1 and 2) opened first and gave way to a nonlinear development of the curvature for these cross sections, whereas the still closed joints (joints 3 and 4) kept the linear relationship between bending moment and curvature. The failure occurred in the cross section of joint 1.

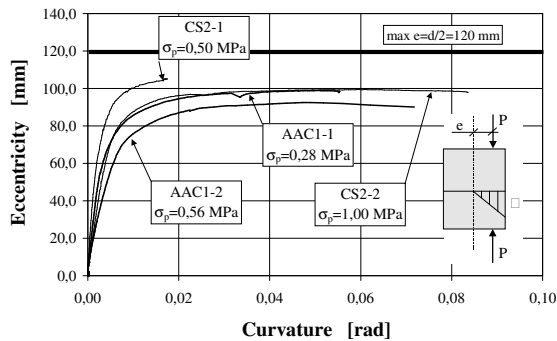


Figure 16 Eccentricity-curvature relationship of prestressed (σ_p) walls

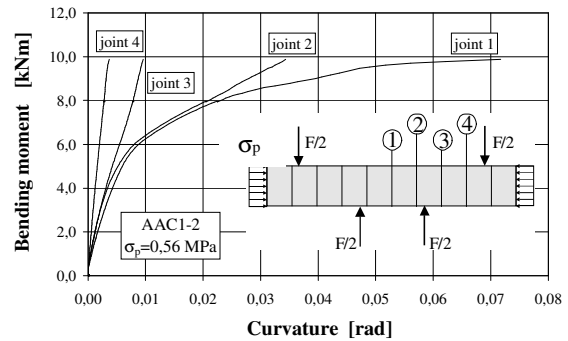


Figure 17 Moment-curvature relationship depending on location of the joint

6 Conclusions

Dry-stacked masonry can bear nearly the same compression loads as traditional masonry with mortar joints. Mortarless masonry develops a different stress-strain relationship than mortared masonry while carrying loads, encompassing an initial joint settlement as well as an elastic degradation of masonry blocks. The failure mechanism is also altered due to the lack of mortar. The shearing and bending capacity are characterized by either sliding along the bed joints, most often connected with a vertical dilatation, or cracking of blocks. If bending generates stresses perpendicular to bed joints, they may be counteracted by post-tensioning, leading to an interaction of bending moment and normal forces.

References

- DIN 18554-1. *Prüfung von Mauerwerk* (Methods of test for masonry). 12/1985 edition.
- DIN EN 1052. *Prüfverfahren für Mauerwerk* (Methods of test for masonry). 07/1993.
- Falkner, H. and Gunkler, E. 1994. Vorgespanntes Mauerwerk (Post-tensioned masonry). *Der Bauingenieur* 69 : 431-437.
- Marzahn, G. 2000, *Untersuchungen zum Trag- und Verformungsverhalten von vorgespanntem Trockenmauerwerk* (Investigation of load bearing and deformation capacity of dry-stacked post-tensioned masonry). PhD-Thesis, University of Leipzig, Leipzig, Germany.